The Ataxia Telangiectasia mutated kinase controls Igκ allelic exclusion by inhibiting secondary *Vκ*-to-*Jκ* rearrangements

Natalie C. Steinel,[1,2,3] Baeck-Seung Lee,[4] Anthony T. Tubbs,[4] Jeffrey J. Bednarski,[5] Emily Schulte,[5] Katherine S. Yang-Iott,[3] David G. Schatz,[6,7] Barry P. Sleckman,[4] and Craig H. Bassing[1,2,3]

[1]Immunology Graduate Group, and [2]Abramson Family Cancer Research Institute, Department of Pathology and Laboratory Medicine, Perelman School of Medicine at the University of Pennsylvania, Philadelphia, PA 19104
[3]Division of Cancer Pathobiology, Department of Pathology and Laboratory Medicine, Center for Childhood Cancer Research, Children's Hospital of Philadelphia, Philadelphia, PA 19104
[4]Department of Pathology and Immunology and [5]Department of Pediatrics, Washington University School of Medicine, St. Louis, MO 63110
[6]Department of Immunobiology, Yale University School of Medicine, New Haven, CT 06520
[7]Howard Hughes Medical Institute, New Haven, CT 06520

Allelic exclusion is enforced through the ability of antigen receptor chains expressed from one allele to signal feedback inhibition of V-to-(D)J recombination on the other allele. To achieve allelic exclusion by such means, only one allele can initiate V-to-(D)J recombination within the time required to signal feedback inhibition. DNA double-strand breaks (DSBs) induced by the RAG endonuclease during V(D)J recombination activate the Ataxia Telangiectasia mutated (ATM) and DNA-dependent protein kinase (DNA-PK) kinases. We demonstrate that ATM enforces Igκ allelic exclusion, and that RAG DSBs induced during *Igκ* recombination in primary pre–B cells signal through ATM, but not DNA-PK, to suppress initiation of additional *Igκ* rearrangements. ATM promotes high-density histone H2AX phosphorylation to create binding sites for MDC1, which functions with H2AX to amplify a subset of ATM-dependent signals. However, neither H2AX nor MDC1 is required for ATM to enforce Igκ allelic exclusion and suppress *Igκ* rearrangements. Upon activation in response to RAG Igκ cleavage, ATM signals down-regulation of Gadd45α with concomitant repression of the Gadd45α targets Rag1 and Rag2. Our data indicate that ATM kinases activated by RAG DSBs during *Igκ* recombination transduce transient H2AX/MDC1-independent signals that suppress initiation of further *Igκ* rearrangements to control Igκ allelic exclusion.

CORRESPONDENCE
Craig H. Bassing:
bassing@email.chop.edu

Abbreviations used: AgR, antigen receptor; ATM, Ataxia Telangiectasia mutated; CE, coding end; CJ, coding join; DSBs, DNA double-strand breaks; DNA-PK, DNA-dependent protein kinase; GL, germline.

Assembly of Ig and TCR genes from variable (V), diversity (D), and joining (J) segments is the pervasive means by which antigen receptor (AgR) diversity is generated (Brady et al., 2010). V(D)J recombination is initiated by the RAG1/RAG2 (RAG) endonuclease that induces DNA double-strand breaks (DSBs) adjacent to participating segments (Schatz and Ji, 2011) and completed by DSB repair factors that process V(D)J coding ends (CEs) into coding joins (CJs; Helmink and Sleckman, 2012). AgR assembly occurs during and is required for lymphocyte differentiation. IgH genes are assembled through D_H-to-J_H recombination, followed by V_H-to-DJ_H rearrangements on one allele at a time in pro–B cells (Rajewsky, 1996). IgH chains expressed from in-frame V_HDJ_H joins can bind λ5/Vpre–B chains to form pre-BCRs that signal inhibition of V_H rearrangements, proliferation, and differentiation into pre–B cells (Rajewsky, 1996). The two-thirds of cells that assemble out-of-frame V_HDJ_H joins can attempt to assemble in-frame V_HDJ_H joins on the second allele (Rajewsky, 1996). Igκ genes are assembled from Vκ and Jκ segments on one allele at a time in G1 phase pre–B cells (Rajewsky, 1996). Igκ chains expressed from VκJκ joins can bind IgH chains to

N.C. Steinel and B.-S. Lee contributed equally to this paper.

The Rockefeller University Press $30.00
J. Exp. Med. 2013 Vol. 210 No. 2 233-239
www.jem.org/cgi/doi/10.1084/jem.20121605

The Journal of Experimental Medicine

form κ+ BCRs that are subject to selection (Rajewsky, 1996; Nemazee, 2006). Non-autoreactive BCRs signal inhibition of Igκ recombination and differentiation into B cells (Nemazee, 2006). Autoreactive BCRs induce additional Igκ rearrangements that replace VκJκ complexes, a process known as Igκ editing (Nemazee, 2006). Pre–B cells that assemble out-of-frame VκJκ joins can attempt to assemble in-frame VκJκ joins on the other allele (Rajewsky, 1996).

Most lymphocytes express surface AgR chains from a single allele. Allelic exclusion is enforced through the ability of Ig and TCR chains expressed from one allele to signal feedback inhibition of V-to-(D)J rearrangements on the second allele (Brady et al., 2010; Vettermann and Schlissel, 2010). To achieve allelic exclusion, only one allele can initiate V-to-(D)J recombination in the time required for feedback inhibition. V-to-(D)J recombination requires CTCF-mediated looping between RAG accessible V segments and RAG-bound D/J segments (Guo et al., 2011; Schatz and Swanson, 2011). In pre–B cells, *Igκ* loci replicate asynchronously and the early replicating allele is preferentially rendered accessible and selected for *Igκ* recombination (Mostoslavsky et al., 2001). The time between replication of *Igκ* loci might be sufficient to enable Igκ chains from the first allele to prevent *Igκ* rearrangements on the second allele. Yet experiments that show Igκ allelic exclusion is enforced by asynchronous replication between *Igκ* alleles have not been reported.

The feedback model for allelic exclusion hypothesized that V(D)J recombination could activate transient intracellular signals that inhibit recombination on the second allele (Alt et al., 1980). RAG DSBs activate DNA-dependent protein kinase (DNA-PK), which forms an endonuclease with Artemis that processes CEs (Ma et al., 2002). RAG DSBs also activate Ataxia Telangiectasia mutated (ATM), which phosphorylates proteins to coordinate the cellular DSB response (Bredemeyer et al., 2006, 2008). In pre–B cells, RAG DSBs signal through ATM to initiate a genetic program that controls differentiation (Bredemeyer et al., 2008). ATM promotes high-density histone H2AX phosphorylation along RAG-cleaved loci (Savic et al., 2009). H2AX phosphorylation creates binding sites for MDC1, which retains activated ATM kinases around DSBs (Lou et al., 2006). The pools of activated ATM bound and not bound to H2AX/MDC1 exhibit different signaling capabilities (Celeste et al., 2002; Lou et al., 2006). In G1 phase cells, ATM promotes CJ formation independent of H2AX and MDC1 (Bredemeyer et al., 2006; Yin et al., 2009; Helmink et al., 2011). H2AX phosphorylation is detectable over only one *Igκ* locus in most pre–B cells including those with paired *Igκ* alleles (Hewitt et al., 2009). The fraction of cells with H2AX phosphorylation over both *Igκ* loci is fivefold higher in $Atm^{-/-}$ mice relative to wild-type mice (Hewitt et al., 2009), suggesting that *Igκ* recombination initiates on a single paired allele and ATM bound to this allele acts on the other allele to prevent bi-allelic rearrangements (Hewitt et al., 2009). Detection of bi-allelic *Igκ* chromosome breaks in *Atm*-deficient pre–B cell lines provided support for this model (Hewitt et al., 2009).

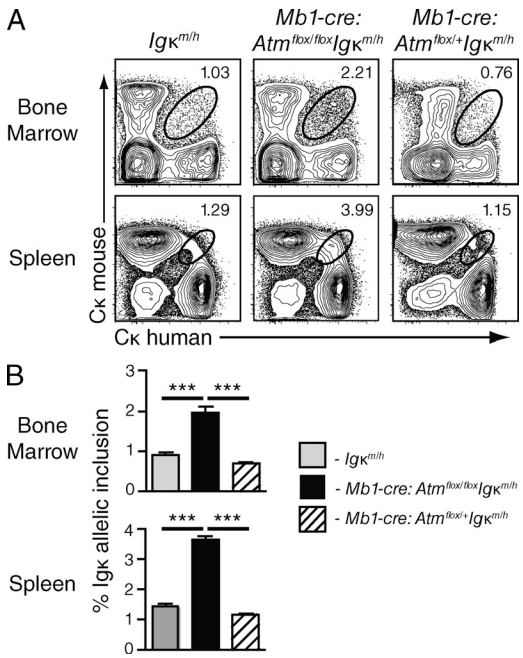

Figure 1. ATM enforces *Igκ* allelic exclusion. (A) Analysis of $Igκ^m$ and $Igκ^h$ expression on bone marrow and splenic B cells isolated from the indicated mice. Shown are the gates used to quantify B cells expressing $Igκ^m$ and $Igκ^h$ at equal high levels and the percentages of cells in these gates. (B) Graph showing the mean frequencies of *Igκ* allelic inclusion in bone marrow and splenic B cells of the indicated mice. Data are from four independent experiments conducted on five $Igκ^{m/h}$, six *Mb1-cre*$Atm^{flox/flox}Igκ^{m/h}$ littermates, and three age-matched *Mb1-cre*$Atm^{flox/+}Igκ^{m/h}$ mice. Error bars are SEM. ***, $P < 0.0001$.

Here, we show in mice that inactivation of ATM causes a higher frequency of B cells expressing surface Igκ chains from both alleles. We show in primary pre–B cells that DSBs induced during *Igκ* recombination signal through ATM, but not DNA-PK, to suppress further *Igκ* rearrangements. Neither H2AX nor MDC1 is required for the ability of ATM to enforce Igκ allelic exclusion or inhibit *Igκ* recombination. Upon activation in response to RAG DSBs, ATM signals down-regulation of Gadd45α with concomitant repression of the Gadd45α targets Rag1 and Rag2. Our data indicate that ATM kinases activated by *Igκ* cleavage transduce transient H2AX/MDC1-independent signals that suppress further *Igκ* rearrangements and thereby enforce Igκ allelic exclusion.

RESULTS AND DISCUSSION

To determine whether ATM enforces Igκ allelic exclusion, we used $Igκ^{m/h}$ mice that express an allotypic marker that enables analysis of surface Igκ expression from each allele using anti-$Igκ^m$ and anti-$Igκ^h$ antibodies (Casellas et al., 2001). Because ~1/3 of CJs are assembled in-frame and Igκ chains are required for differentiation, 20% is the maximal frequency of B cells that can exhibit Igκ allelic inclusion, assuming simultaneous Igκ rearrangements on both alleles and no Igκ feedback inhibition and selection for/against dual-$Igκ^+$ cells (Alt et al., 1984). However, as a result of the CJ formation defect in $Atm^{-/-}$ cells (Bredemeyer et al., 2006), <20% of *Atm*-deficient

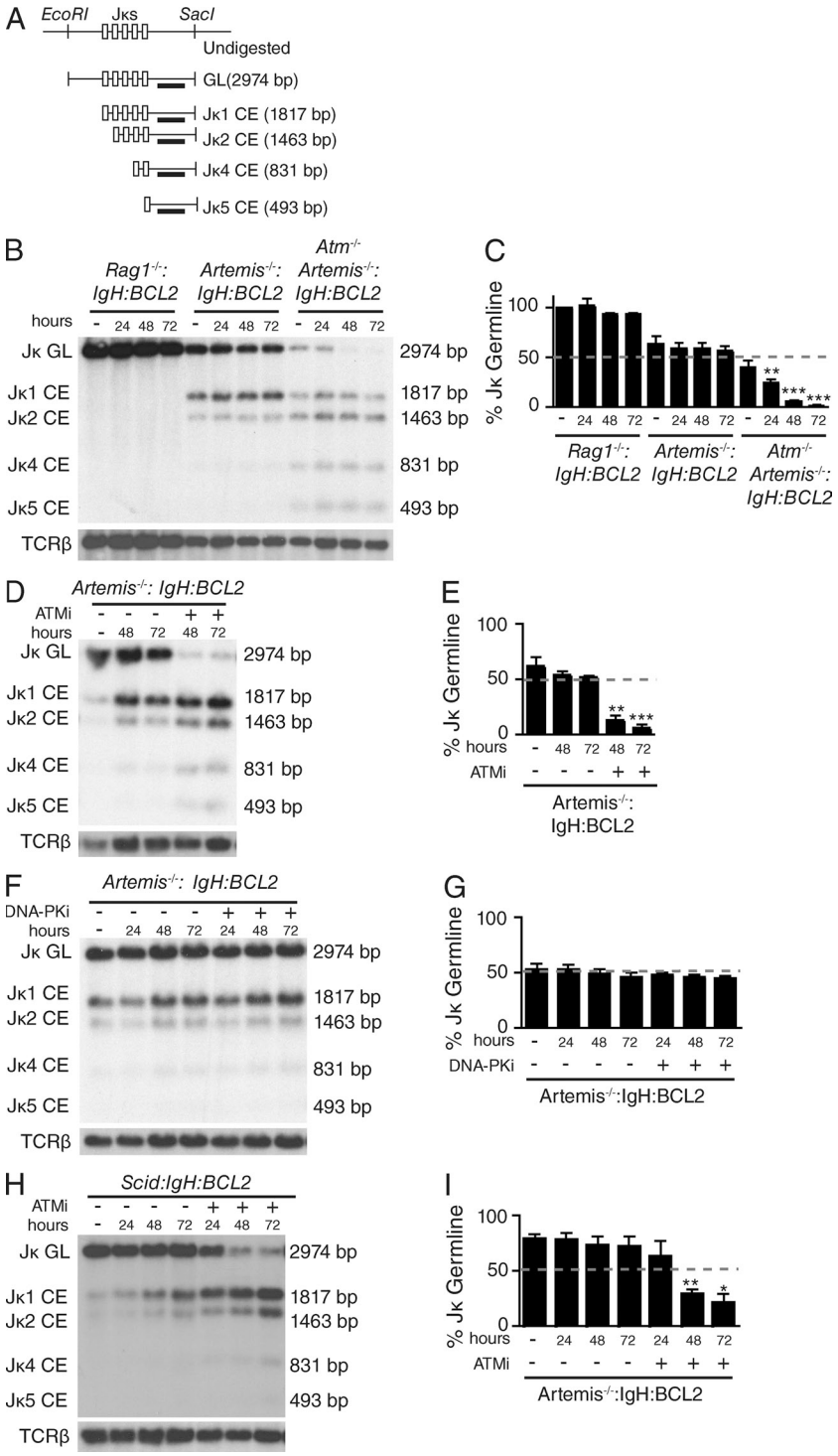

Figure 2. ATM inhibits *Igκ* cleavage. (A) Schematic of the GL *Jκ* locus and EcoR1/SacI fragments of *Jκ* loci in GL configuration or with CEs for the functional *Jκ*s. Indicated are the sizes of the restriction fragments and the probe used to visualize these. (B–I) Southern blot analyses (B, D, G, and H) and quantification of Jκ cleavage (C, E, G, and I) in the indicated pre–B cells before and at indicated times after IL7 removal or IL7 removal and KU55933 addition. GL *Jκ* loci and *Jκ* CE bands are labeled. Southern blots with a *TCRβ* probe for DNA content are also shown. Data are from three independent experiments. Error bars represent SEM. Asterisks (*, P = 0.05–0.01; **, P = 0.001–0.01; ***, P < 0.0001) indicate Jκ cleavage that is significant from the comparable time in untreated *Artemis*$^{-/-}$*:IgH:BCL2* (C, E, and G) or *Scid:IgH:BCL2* (I) cells.

Igκ$^{m/h}$ B cells should express surface Igκ chains from both alleles if ATM controls Igκ allelic exclusion. Because a small fraction of *Igκ*$^{m/h}$ B cells exhibits Igκ allelic inclusion (Casellas et al., 2001;Velez et al., 2007; Fournier et al., 2012), we bred *Igκ*$^{m/h}$ and *Mb1-creAtm*$^{flox/flox}$ mice to more readily generate *Mb1-creAtm*$^{flox/flox}$*Igκ*$^{m/h}$ mice with B lineage–specific Atm inactivation and littermate control *Atm*$^{flox/flox}$*Igκ*$^{m/h}$ mice (frequency of 0.5) compared with *Atm*$^{-/-}$*Cκ*$^{h/m}$ and *Atm*$^{+/+}$*Cκ*$^{h/m}$ littermate mice (frequency of 0.25). We observed equal high-level expression of Igκ^{m} and Igκ^{h} on 1.98 ± 0.14% of bone marrow and 3.68 ± 0.10% of splenic B cells from *Mb1-creAtm*$^{flox/flox}$*Igκ*$^{m/h}$ mice (Fig. 1). The frequencies of cells expressing high levels of surface Igκ^{m} and Igκ^{h} were ∼2.5-fold greater in *Mb1-creAtm*$^{flox/flox}$*Igκ*$^{m/h}$ mice as compared with

littermate $Ig\kappa^{m/h}$ mice (bone marrow: 0.92 ± 0.04 vs. 1.98 ± 0.14%, P < 0.0001; spleen: 1.48 ± 0.06 vs. 3.68 ± 0.10%, P < 0.0001) and age-matched $Mb1\text{-}creAtm^{flox/+}Ig\kappa^{m/h}$ mice (Fig. 1). These data demonstrate that Igκ allelic exclusion is not enforced as strictly in Atm-deficient B cells.

Less strict enforcement of Igκ allelic exclusion could be a result of loss of signals that coordinate initiation of *Igκ* rearrangements between alleles and/or slower CJ formation on the first allele that leads to initiation of *Igκ* recombination on the second allele before feedback inhibition. To assess if ATM enforces Igκ allelic exclusion by transducing signals from RAG DSBs on one allele to suppress recombination on the other allele, we needed to quantify initiation of *Igκ* rearrangements independent of ATM functions in CJ formation. For this purpose, we used an approach that we developed to elucidate responses to RAG DSBs in primary pre–B cells (Bednarski et al., 2012). We generated $Rag1^{-/-}$ or $Artemis^{-/-}$ mice expressing IgH and BCL2 transgenes ($Rag1^{-/-}$*:IgH:BCL2* and $Artemis^{-/-}$*:IgH:BCL2* mice); these mice each exhibit a block in B cell development at the pre–B cell stage caused by inability to assemble *Igκ* genes (Bednarski et al., 2012).

Southern analysis of *Jκ* cleavage can be used to quantify initiation of *Igκ* rearrangements (Fig. 2 A). Because IL7 promotes pre–B cell proliferation and represses *Igκ* accessibility and RAG expression (Billips et al., 1995; Amin and Schlissel, 2008; Johnson et al., 2008; Malin et al., 2010), culturing $Rag1^{-/-}$*:IgH:BCL2* or $Artemis^{-/-}$*:IgH:BCL2* bone marrow in IL7 leads to outgrowth of pre–B cells with germline (GL) *Igκ* loci (Fig. 2 B). Yet a fraction of IL7-cultured $Artemis^{-/-}$*:IgH:BCL2* cells accumulates *Igκ* CEs because IL7 does not block *Igκ* accessibility and RAG expression (Fig. 2 B). Removal of $Rag1^{-/-}$*:IgH:BCL2* or $Artemis^{-/-}$*:IgH:BCL2* cells from IL7 leads to G1 arrest and stimulation of Igκ accessibility and RAG expression (Bednarski et al., 2012); $Rag1^{-/-}$*:IgH:BCL2* cells retain GL *Igκ* loci, whereas $Artemis^{-/-}$*:IgH:BCL2* cells lose GL *Igκ* loci and accumulate *Jκ1* and *Jκ2* CEs (Fig. 2, B and C). These Igκ DSBs activate ATM-mediated signals, as indicated by phosphorylation of p53 after removal of $Artemis^{-/-}$*:IgH:BCL2* but not $Rag1^{-/-}$*:IgH:BCL2* cells from IL7 and by inhibition of these responses by the KU55933 ATM kinase inhibitor (Bednarski et al., 2012).

Because CEs are not processed into CJs in $Artemis^{-/-}$*:IgH:BCL2* cells (Bednarski et al., 2012), these cells enable us to assess if ATM signals inhibition of *Igκ* recombination independent of ATM function in CJ formation. We grew $Artemis^{-/-}$*:IgH:BCL2* pre–B cells in IL7, removed IL7, placed cells back into culture in the absence or presence of KU55933, isolated DNA at 0, 48, and 72 h after IL7 removal, and then conducted Southern blots. We detected GL *Jκ* loci and a low level of *Jκ1* CEs in IL7-cultured cells (Fig. 2, D and E). At 48 and 72 h after IL7 removal, we observed decreased GL *Jκ* loci, increased levels of *Jκ1* CEs, and appearance of *Jκ2* CEs (Fig. 2, D and E). In contrast, at 48 and 72 h after IL7 removal and KU55933 addition, we detected near loss of GL *Jκ* loci, higher levels of *Jκ1* CEs, and appearance of *Jκ2*, *Jκ4*, and *Jκ5* CEs (Fig. 2, D and E). To rule out off-target KU55933 effects, we

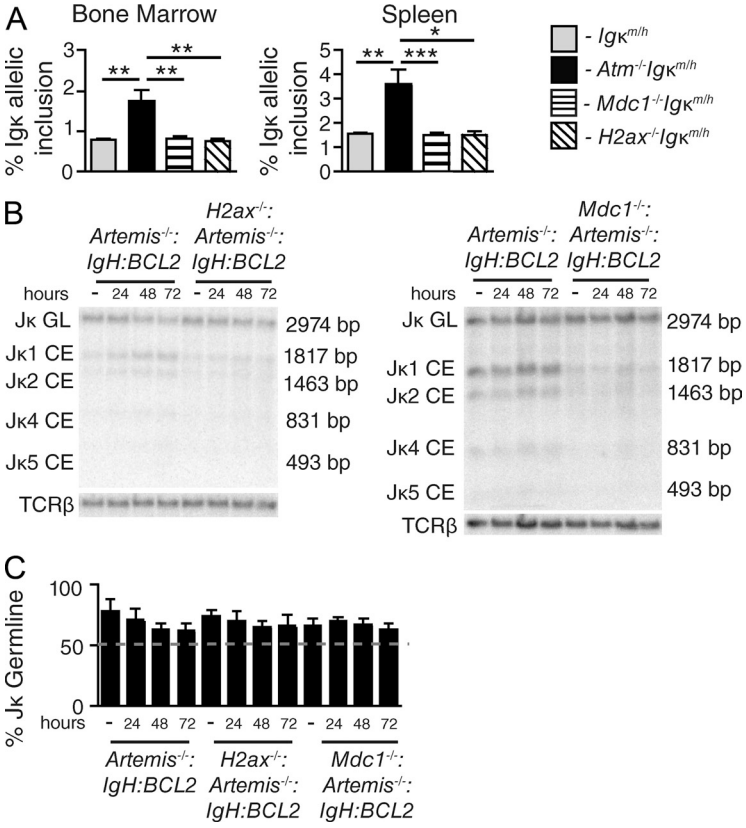

Figure 3. ATM controls Igκ recombination and allelic exclusion independent of H2AX and MDC1. (A) Graphs showing the mean frequencies of *Igκ* allelic inclusion in bone marrow and splenic B cells isolated from the indicated mice. Data are from at least three independent experiments conducted on five $Ig\kappa^{m/h}$ mice, three $Atm^{-/-}Ig\kappa^{m/h}$, six $H2ax^{-/-}Ig\kappa^{m/h}$, and seven $Mdc1^{-/-}Ig\kappa^{m/h}$ age-matched mice. Error bars represent SEM. *, P = 0.05–0.01; **, P = 0.001–0.01; ***, P < 0.001. (B and C) Southern analyses (B) and graphs showing quantification (C) of Jκ cleavage in the indicated pre–B cells before and at indicated times after IL7 withdrawal. GL *Jκ* loci and *Jκ* CE bands are labeled. Southern blots with a *TCRβ* probe for DNA content are also shown. Data are from three independent experiments conducted on four $Artemis^{-/-}$*:IgH:BCL2*, three $H2ax^{-/-}Artemis^{-/-}$*:IgH:BCL2*, and two $Mdc1^{-/-}Artemis^{-/-}$*:IgH:BCL2* cultures. $Artemis^{-/-}$*:IgH:BCL2* and $H2ax^{-/-}Artemis^{-/-}$*:IgH:BCL2* error bars represent SEM and $Mdc1^{-/-}Artemis^{-/-}$*:IgH:BCL2* error bars represent SD.

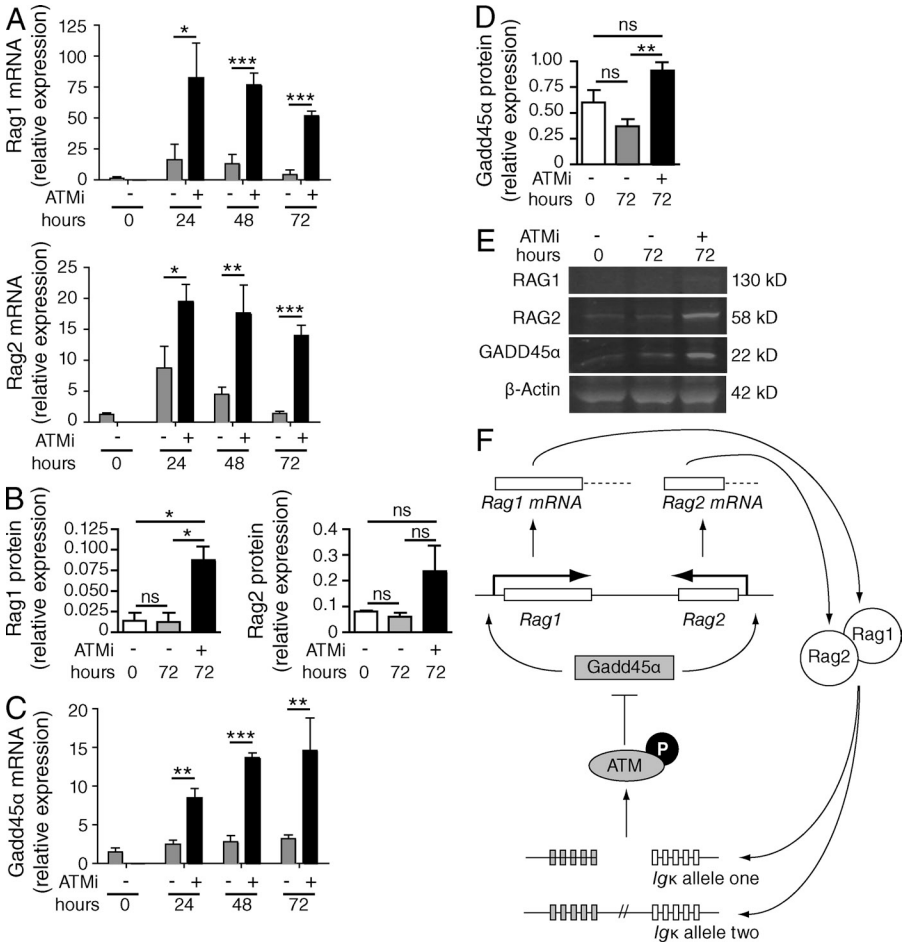

Figure 4. ATM represses RAG expression. (A and B) Graphs showing the mean levels of Rag1 or Rag2 mRNA (A) or protein (B) relative to β-actin mRNA or protein in *Artemis*$^{-/-}$*:IgH:BCL2* cells before and at indicated times after IL7 withdrawal or IL7 withdrawal and addition of ATM inhibitor KU55933. (C and D) Graphs showing the mean levels of Gadd45α mRNA (C) or protein (D) relative to β-actin mRNA or protein in *Artemis*$^{-/-}$*:IgH:BCL2* cells before and at indicated times after IL7 withdrawal or IL7 withdrawal and KU55933 addition. (A–D) Data were generated from three independent experiments. Error bars represent SEM. *, $P < 0.05$; **, $P < 0.01$; ***, $P < 0.001$. (E) Western blot data from an experiment in B and D. (F) Model showing how the ATM-dependent RAG negative feedback loop suppresses further Igκ rearrangements on either allele to control Igκ allelic exclusion and ensure broad utilization of Jκ segments in selected Igκ chains.

analyzed *Jκ* cleavage in *Atm*$^{-/-}$*:Artemis*$^{-/-}$*:IgH:BCL2* cells. As compared with IL7-cultured *Artemis*$^{-/-}$*:IgH:BCL2* cells, we found fewer GL *Jκ* loci and higher levels of *Jκ* CEs in *Atm*$^{-/-}$*:Artemis*$^{-/-}$*:IgH:BCL2* cells cultured in IL7 (Fig. 2, B and C). We detected near complete loss of GL *Jκ* loci and increased levels of *Jκ4* and *Jκ5* CEs after IL7 removal from *Atm*$^{-/-}$*:Artemis*$^{-/-}$*:IgH:BCL2* cells (Fig. 2, B and C). The relative levels of GL *Jκ* loci and *Jκ* CEs indicate that RAG DSBs were induced on roughly half the *Igκ* alleles in *Artemis*$^{-/-}$*:IgH:BCL2* cells, and on almost all *Jκ* alleles in the absence of ATM. These data show that RAG DSBs induced during *Igκ* recombination signal through ATM to suppress initiation of further *Igκ* rearrangements.

Because DNA-PK is activated by DSBs, we also assessed if DNA-PK inhibits *Igκ* recombination. We observed no changes in levels of GL *Jκ* loci or *Jκ* CEs after IL7 withdrawal of *Artemis*$^{-/-}$*:IgH:BCL2* cells in the presence or absence of the NU7026 DNA-PK kinase inhibitor (Fig. 2, F and G). Because Artemis phosphorylation by DNA-PK is required for CJs (Ma et al., 2002), *Scid* cells that lack DNA-PK are equal to *Artemis*$^{-/-}$ cells with respect to CE accumulation (Savic et al., 2009). We observed similar loss of GL *Jκ* loci and elevated levels of *Jκ1* and *Jκ2* CEs after IL7 removal from *Scid:IgH:BCL2* cells (Fig. 2, H and I), relative to *Artemis*$^{-/-}$*:IgH:BCL2* cells (Fig. 2, B and C). Yet we detected near loss of GL *Jκ* loci, increased levels of *Jκ1* and *Jκ2* CEs, and appearance of *Jκ4* CEs after IL7 removal and KU55933 addition to *Scid:IgH:BCL2* cells (Fig. 2 H, I). These data demonstrate that ATM, but not DNA-PK, transduces signals that inhibit *Igκ* rearrangements.

H2ax$^{-/-}$ and *Mdc1*$^{-/-}$ cells exhibit impaired ATM-mediated activation of some checkpoints (Lou et al., 2006) but normal ATM-mediated activation of other checkpoints (Celeste et al., 2002), indicating that the pools of ATM bound and not bound to H2AX/MDC1 exhibit different signaling capabilities. To determine if the ATM kinases bound to H2AX/MDC1 along RAG-cleaved *Igκ* loci enforce Igκ allelic exclusion, we analyzed *Igκ*$^{m/h}$, *Atm*$^{-/-}$*Igκ*$^{m/h}$, *H2ax*$^{-/-}$*Igκ*$^{m/h}$, and *Mdc1*$^{-/-}$*Igκ*$^{m/h}$ mice. We found equal high levels of Igκ^{m} and Igκ^{h} expression on bone marrow and splenic B cells from *Igκ*$^{m/h}$, *H2ax*$^{-/-}$*Igκ*$^{m/h}$, and *Mdc1*$^{-/-}$*Igκ*$^{m/h}$ mice (Fig. 3 A). The frequencies of cells exhibiting Igκ allelic inclusion in *H2ax*$^{-/-}$*Igκ*$^{m/h}$ and *Mdc1*$^{-/-}$*Igκ*$^{m/h}$ mice were lower than in *Atm*$^{-/-}$*Igκ*$^{m/h}$ mice (Fig. 3 A). To assess whether the soluble pool of activated ATM kinases controls initiation of *Igκ* rearrangements between alleles, we analyzed *Jκ* cleavage in *Artemis*$^{-/-}$*:IgH:BCL2*, *H2ax*$^{-/-}$*:Artemis*$^{-/-}$*:IgH:BCL2*, and *Mdc1*$^{-/-}$*:Artemis*$^{-/-}$*:IgH:BCL2* pre–B cells. Because H2AX and MDC1

protect CEs from degradation (Helmink et al., 2011), we quantified *Igκ* cleavage by calculating loss of GL *Jκ* band intensity relative to DNA content. We found that cleavage occurred on roughly half of the *Igκ* alleles in *Artemis*$^{-/-}$*:IgH:BCL2*, *H2ax*$^{-/-}$*:Artemis*$^{-/-}$*:IgH:BCL2*, and *Mdc1*$^{-/-}$*:Artemis*$^{-/-}$*:IgH:BCL2* cells (Fig. 3, B and C) rather than on almost all *Igκ* alleles as observed in *Atm*$^{-/-}$*:Artemis*$^{-/-}$*:IgH:BCL2* cells (Fig. 2 C). These data demonstrate that ATM kinases activated by *Igκ* cleavage transduce H2AX/MDC1-independent signals that suppress further *Igκ* rearrangements and thereby enforce Igκ allelic exclusion.

We previously showed that RAG DSBs signal through ATM to increase levels of many mRNAs, including several encoding lymphocyte-specific proteins (Bredemeyer et al., 2008). To test if RAG DSBs signal through ATM to decrease expression of proteins necessary for *Igκ* recombination, we quantified *Rag1* and *Rag2* mRNA and protein in *Artemis*$^{-/-}$*:IgH:BCL2* cells before and after IL7 removal, both in the absence or presence of KU55933. We found that ATM inhibition led to greater levels of *Rag1* and *Rag2* mRNA and protein after IL7 removal (Fig. 4, A, B, and E). In pre–B cells, the Gadd45α stress-regulated protein transduces signals that promote *Rag1/Rag2* transcription and maintain basal RAG expression (Amin and Schlissel, 2008). We found that ATM inhibition also led to higher levels of Gadd54α mRNA and protein after IL7 removal and accumulation of Jκ CEs in *Artemis*$^{-/-}$*:IgH:BCL2* cells (Fig. 4, C, D, and E). These data demonstrate that RAG DSBs induced in pre–B cells activate and signal through ATM kinases to transcriptionally downregulate RAG expression.

We conclude that ATM controls *Igκ* recombination and allelic exclusion through a negative feedback loop. Initial RAG cleavage on the early replicating *Igκ* allele induces ATM-dependent signals that repress RAG activity to provide time for selection of *Igκ* genes before further *Igκ* recombination on either allele. This mechanism would inhibit additional *Igκ* recombination on both alleles regardless of *Igκ* locus positioning. Non-autoreactive BCRs would signal RAG repression and feedback inhibition to enforce Igκ allelic exclusion (Nemazee, 2006), whereas autoreactive BCRs would induce RAG expression and additional Igκ rearrangements on either allele to promote Igκ editing and cause Igκ allelic inclusion (Casellas et al., 2001). ATM inactivation after assembly of out-of-frame CJs would lead to RAG reexpression and reinitiation of *Igκ* recombination on either allele. In addition to controlling allelic exclusion, the ability of ATM to repress RAG activity in response to RAG cleavage likely slows initiation of secondary Igκ rearrangements to ensure broad utilization of Jκ segments in selected Igκ chains. This ATM-dependent negative feedback loop also likely enforces IgH and TCR-β allelic exclusion, ensures broad utilization of D/J segments in other AgR chains, and controls recombination among loci in pro–T cells. ATM also functions in a negative feedback loop to repress the SPO11 endonuclease and limit the number of DSBs during meiosis (Lange et al., 2011), suggesting that pressure to regulate DSB induction during programmed recombination events selected for the evolution of ATM-dependent mechanisms that feedback inhibit tissue-specific nuclease activity.

MATERIALS AND METHODS

Mice. All mice were bred and housed under specific pathogen-free conditions at the Children's Hospital of Philadelphia or the Washington University School of Medicine. All mice were on a 129/B6 mixed background. All analyses were conducted on littermate or age-matched mice. All experiments were performed in accordance with national guidelines and regulations and approved by the Institutional Animal Care and Use Committees of both institutes.

Primary pre–B cell culture. Bone marrow cells were harvested from 4–6-wk-old mice and cultured in media containing IL7 at 5 ng/ml for 7–10 d at 2×10^6 cells/ml. For IL7 withdrawal experiments, cells were harvested, washed in PBS, resuspended, and maintained at 2×10^6 cells/ml in IL7-free media in the presence or absence of 15 μM ATM (KU-55933; Sigma-Aldrich) or 20 μM DNA-PKs (NU7026; Sigma-Aldrich) inhibitors.

Southern blots. Southern blot analyses of RAG Igκ cleavage were performed as previously described (Bednarski et al., 2012). Quantification of loss of *Igκ* GL bands was conducted using ImageJ software (National Institutes of Health) and referenced to *TCRβ* loading control bands.

Flow cytometric analysis. Cells isolated from the bone marrow and spleens of 6–8-wk-old mice were stained with the following antibodies: APC/Cy7 anti–mouse B220 (RA3-6B2; BD), APC anti–mouse TCR-β (H57-597; BD), PE anti–mouse κ (187.1; BD), and biotin anti–human κ (SouthernBiotech). Cell suspensions were depleted of red blood cells with NH_4Cl lysis buffer and stained in PBS containing 3% FCS and 0.25 mM EDTA. Before staining, FC receptors were blocked using anti-CD16/CD32 (2.4G2; BD). Data were collected on an LSR II and analyzed with FlowJo software (Tree Star). Surface Igκ expression was assayed on single, DAPI$^-$, TCR-β$^-$, and B220$^+$ cells. Single, live cells were gated on the basis of forward and side scatter and DAPI exclusion (D1306; Invitrogen).

qRT-PCR. RNA was isolated as previously described (Bednarski et al., 2012). Each reaction was run in triplicate. Rag1 and Rag2 mRNA levels were normalized to β-actin mRNA levels. The primers used were: Rag1 forward, 5′-TGGGAATCGTTTCAAGAGTGAC-3′, and Rag1 reverse, 5′-CATCTGCCTTCACGTCGATCC-3′; Rag2 forward, 5′-ACACCAAACAATGAGCTTTCCG-3′, and Rag2 reverse, 5′-CCGTATCTGGGTTCAGGGAC-3′; Gadd45α forward, 5′-CCGAAAGGATGGACACGGTG-3′, and Gadd45α reverse, 5′-TTATCGGGGTCTACGTTGAGC-3′; or β-actin forward, 5′-TCATCACTATTGGCAACGAGCGGTTC-3′, and β-actin reverse, 5′-TACCACCAGACAGCACTGTGTTGGCA-3′.

Western blots. Whole cell lysates isolated from 30×10^6 IL7 withdrawn pre–B cells were run on 10% Tris-Glycine gels (Novex), transferred to PVDF membrane (Immobilon; Millipore), blocked in Odyssey Blocking Buffer (LI-COR Biosciences) and probed with the following monoclonal antibodies: rabbit anti–mouse Rag1 #23 and rabbit anti–mouse Rag2 #39 (Coster et al., 2012), rabbit anti–mouse Gadd45α (D17E8; Cell Signaling Technology), rabbit anti–mouse β-actin (Sigma-Aldrich), and IRDye 800CW goat anti–rabbit IgG (LI-COR Biosciences). Western blots were visualized and quantified using the Odyssey Infrared Imaging System (LI-COR Biosciences). Rag1, Rag2, and Gadd45α protein levels were normalized to β-actin protein levels.

Statistical analyses. All p-values were generated by Student's *t* test using Prism (GraphPad Software).

This research was supported by a Cancer Research Institute Pre-doctoral Emphasis Pathway in Tumor Immunology Training Grant (N.C. Steinel), a Hyundai Scholars Award (J.J. Bednarski), a Leukemia and Lymphoma Scholar Award (C.H. Bassing), and the National

Institutes of Health Grants K08AI102946 (J.J. Bednarski), R37 AI32524 (D.G. Schatz), R01 CA125195 (C.H. Bassing), and R01 CA136470 (C.H. Bassing and B.P. Sleckman).

The authors have no conflicting financial interests to declare.

Submitted: 19 July 2012
Accepted: 9 January 2013

REFERENCES

Alt, F.W., V. Enea, A.L.M. Bothwell, and D. Baltimore. 1980. Activity of multiple light chain genes in murine myeloma cells producing a single, functional light chain. *Cell*. 21:1–12. http://dx.doi.org/10.1016/0092-8674(80)90109-9

Alt, F.W., G.D. Yancopoulos, T.K. Blackwell, C. Wood, E. Thomas, M. Boss, R. Coffman, N. Rosenberg, S. Tonegawa, and D. Baltimore. 1984. Ordered rearrangement of immunoglobulin heavy chain variable region segments. *EMBO J.* 3:1209–1219.

Amin, R.H., and M.S. Schlissel. 2008. Foxo1 directly regulates the transcription of recombination-activating genes during B cell development. *Nat. Immunol.* 9:613–622. http://dx.doi.org/10.1038/ni.1612

Bednarski, J.J., A. Nickless, D. Bhattacharya, R.H. Amin, M.S. Schlissel, and B.P. Sleckman. 2012. RAG-induced DNA double-strand breaks signal through Pim2 to promote pre-B cell survival and limit proliferation. *J. Exp. Med.* 209:11–17. http://dx.doi.org/10.1084/jem.20112078

Billips, L.G., C.A. Nuñez, F.E. Bertrand III, A.K. Stankovic, G.L. Gartland, P.D. Burrows, and M.D. Cooper. 1995. Immunoglobulin recombinase gene activity is modulated reciprocally by interleukin 7 and CD19 in B cell progenitors. *J. Exp. Med.* 182:973–982. http://dx.doi.org/10.1084/jem.182.4.973

Brady, B.L., N.C. Steinel, and C.H. Bassing. 2010. Antigen receptor allelic exclusion: an update and reappraisal. *J. Immunol.* 185:3801–3808. http://dx.doi.org/10.4049/jimmunol.1001158

Bredemeyer, A.L., G.G. Sharma, C.Y. Huang, B.A. Helmink, L.M. Walker, K.C. Khor, B. Nuskey, K.E. Sullivan, T.K. Pandita, C.H. Bassing, and B.P. Sleckman. 2006. ATM stabilizes DNA double-strand-break complexes during V(D)J recombination. *Nature*. 442:466–470. http://dx.doi.org/10.1038/nature04866

Bredemeyer, A.L., B.A. Helmink, C.L. Innes, B. Calderon, L.M. McGinnis, G.K. Mahowald, E.J. Gapud, L.M. Walker, J.B. Collins, B.K. Weaver, et al. 2008. DNA double-strand breaks activate a multi-functional genetic program in developing lymphocytes. *Nature*. 456:819–823. http://dx.doi.org/10.1038/nature07392

Casellas, R., T.A. Shih, M. Kleinewietfeld, J. Rakonjac, D. Nemazee, K. Rajewsky, and M.C. Nussenzweig. 2001. Contribution of receptor editing to the antibody repertoire. *Science*. 291:1541–1544. http://dx.doi.org/10.1126/science.1056600

Celeste, A., S. Petersen, P.J. Romanienko, O. Fernandez-Capetillo, H.T. Chen, O.A. Sedelnikova, B. Reina-San-Martin, V. Coppola, E. Meffre, M.J. Difilippantonio, et al. 2002. Genomic instability in mice lacking histone H2AX. *Science*. 296:922–927. http://dx.doi.org/10.1126/science.1069398

Coster, G., A. Gold, D. Chen, D.G. Schatz, and M. Goldberg. 2012. A dual interaction between the DNA damage response protein MDC1 and the RAG1 subunit of the V(D)J recombinase. *J. Biol. Chem.* 287:36488–36498. http://dx.doi.org/10.1074/jbc.M112.402487

Fournier, E.M., M.G. Velez, K. Leahy, C.L. Swanson, A.V. Rubtsov, R.M. Torres, and R. Pelanda. 2012. Dual-reactive B cells are autoreactive and highly enriched in the plasmablast and memory B cell subsets of autoimmune mice. *J. Exp. Med.* 209:1797–1812. http://dx.doi.org/10.1084/jem.20120332

Guo, C., H.S. Yoon, A. Franklin, S. Jain, A. Ebert, H.L. Cheng, E. Hansen, O. Despo, C. Bossen, C. Vettermann, et al. 2011. CTCF-binding elements mediate control of V(D)J recombination. *Nature*. 477:424–430. http://dx.doi.org/10.1038/nature10495

Helmink, B.A., and B.P. Sleckman. 2012. The response to and repair of RAG-mediated DNA double-strand breaks. *Annu. Rev. Immunol.* 30:175–202. http://dx.doi.org/10.1146/annurev-immunol-030409-101320

Helmink, B.A., A.T. Tubbs, Y. Dorsett, J.J. Bednarski, L.M. Walker, Z. Feng, G.G. Sharma, P.J. McKinnon, J. Zhang, C.H. Bassing, and B.P. Sleckman. 2011. H2AX prevents CtIP-mediated DNA end resection and aberrant repair in G1-phase lymphocytes. *Nature*. 469:245–249. http://dx.doi.org/10.1038/nature09585

Hewitt, S.L., B. Yin, Y. Ji, J. Chaumeil, K. Marszalek, J. Tenthorey, G. Salvagiotto, N. Steinel, L.B. Ramsey, J. Ghysdael, et al. 2009. RAG-1 and ATM coordinate monoallelic recombination and nuclear positioning of immunoglobulin loci. *Nat. Immunol.* 10:655–664. http://dx.doi.org/10.1038/ni.1735

Johnson, K., T. Hashimshony, C.M. Sawai, J.M. Pongubala, J.A. Skok, I. Aifantis, and H. Singh. 2008. Regulation of immunoglobulin light-chain recombination by the transcription factor IRF-4 and the attenuation of interleukin-7 signaling. *Immunity*. 28:335–345. http://dx.doi.org/10.1016/j.immuni.2007.12.019

Lange, J., J. Pan, F. Cole, M.P. Thelen, M. Jasin, and S. Keeney. 2011. ATM controls meiotic double-strand-break formation. *Nature*. 479:237–240. http://dx.doi.org/10.1038/nature10508

Lou, Z., K. Minter-Dykhouse, S. Franco, M. Gostissa, M.A. Rivera, A. Celeste, J.P. Manis, J. van Deursen, A. Nussenzweig, T.T. Paull, et al. 2006. MDC1 maintains genomic stability by participating in the amplification of ATM-dependent DNA damage signals. *Mol. Cell.* 21:187–200. http://dx.doi.org/10.1016/j.molcel.2005.11.025

Ma, Y., U. Pannicke, K. Schwarz, and M.R. Lieber. 2002. Hairpin opening and overhang processing by an Artemis/DNA-dependent protein kinase complex in nonhomologous end joining and V(D)J recombination. *Cell.* 108:781–794. http://dx.doi.org/10.1016/S0092-8674(02)00671-2

Malin, S., S. McManus, C. Cobaleda, M. Novatchkova, A. Delogu, P. Bouillet, A. Strasser, and M. Busslinger. 2010. Role of STAT5 in controlling cell survival and immunoglobulin gene recombination during pro-B cell development. *Nat. Immunol.* 11:171–179. http://dx.doi.org/10.1038/ni.1827

Mostoslavsky, R., N. Singh, T. Tenzen, M. Goldmit, C. Gabay, S. Elizur, P. Qi, B.E. Reubinoff, A. Chess, H. Cedar, and Y. Bergman. 2001. Asynchronous replication and allelic exclusion in the immune system. *Nature*. 414:221–225. http://dx.doi.org/10.1038/35102606

Nemazee, D. 2006. Receptor editing in lymphocyte development and central tolerance. *Nat. Rev. Immunol.* 6:728–740. http://dx.doi.org/10.1038/nri1939

Rajewsky, K. 1996. Clonal selection and learning in the antibody system. *Nature*. 381:751–758. http://dx.doi.org/10.1038/381751a0

Savic, V., B. Yin, N.L. Maas, A.L. Bredemeyer, A.C. Carpenter, B.A. Helmink, K.S. Yang-Iott, B.P. Sleckman, and C.H. Bassing. 2009. Formation of dynamic γ-H2AX domains along broken DNA strands is distinctly regulated by ATM and MDC1 and dependent upon H2AX densities in chromatin. *Mol. Cell.* 34:298–310. http://dx.doi.org/10.1016/j.molcel.2009.04.012

Schatz, D.G., and Y. Ji. 2011. Recombination centres and the orchestration of V(D)J recombination. *Nat. Rev. Immunol.* 11:251–263. http://dx.doi.org/10.1038/nri2941

Schatz, D.G., and P.C. Swanson. 2011. V(D)J recombination: mechanisms of initiation. *Annu. Rev. Genet.* 45:167–202. http://dx.doi.org/10.1146/annurev-genet-110410-132552

Velez, M.G., M. Kane, S. Liu, S.B. Gauld, J.C. Cambier, R.M. Torres, and R. Pelanda. 2007. Ig allotypic inclusion does not prevent B cell development or response. *J. Immunol.* 179:1049–1057.

Vettermann, C., and M.S. Schlissel. 2010. Allelic exclusion of immunoglobulin genes: models and mechanisms. *Immunol. Rev.* 237:22–42. http://dx.doi.org/10.1111/j.1600-065X.2010.00935.x

Yin, B., V. Savic, M.M. Juntilla, A.L. Bredemeyer, K.S. Yang-Iott, B.A. Helmink, G.A. Koretzky, B.P. Sleckman, and C.H. Bassing. 2009. Histone H2AX stabilizes broken DNA strands to suppress chromosome breaks and translocations during V(D)J recombination. *J. Exp. Med.* 206:2625–2639. http://dx.doi.org/10.1084/jem.20091320